EFFECTS OF GRAPHENE OXIDE ON MOLECULAR DYNAMICS, THERMAL AND MECHANICAL PROPERTIES OF POLY(L-LACTIC ACID)

P. Klonos[1], G.Z. Papageorgiou[2], Z. Terzopoulou[2], S.K. Triantafyllidis[2], D. Gournis[3], D.N. Bikiaris[2], A. Kyritsis[1], P. Pissis [1,*]

[1]*Physics Department, National Technical University of Athens, Zografou, 15780, Athens, Greece*
[2]*Department of Chemistry, Aristotle University of Thessaloniki, GR-54124, Thessaloniki, Greece*
[3]*Department of Materials Science and Engineering, University of Ioannina, GR-45110, Ioannina, Greece*
*e-mail of the corresponding author ppissis@cental.ntua.gr

Keywords: Polymer-matrix composites; Interfaces; Thermomechanical properties; Graphene.

Abstract
Graphene oxide (GO) and graphene oxide modified with dodecylamine (org-GO) were combined with poly(L-lactic acid) (PLLA) to prepare new nanocomposites. A variety of experimental techniques were employed to study structure and morphology, thermal transitions, molecular mobility, mechanical properties, and biodegradation. Results showed that in the nanocomposites GO and org-GO were exfoliated, crystallization was accelerated, the degree of crystallinity was increased, and biodegradation rates were enhanced. Reduction of the dielectric strength of the segmental relaxation associated with the glass transition in the nanocomposites suggests strong polymer-filler interactions and correlates well with the reduction of the heat capacity jump at the glass transition observed by DSC and the improvement of mechanical properties of PLLA after addition of GO and org-GO.

1. Introduction

Interest in biodegradable polymers is high because of their wide use for biomedical, drug delivery, and packaging applications [1]. PLLA is a most promising polymer, known for its satisfying physicochemical properties, possibility of producing from renewable resources, degradability to natural products in a short period of time (0.5–2 years) [2, 3]. For some applications, however, PLLA requires modification. The enhancement of thermal stability, mechanical and barrier properties of PLLA can be achieved by adding nanofillers [4, 5].

Graphene is an exciting material with a wide variety of potential applications [6]. Graphite oxide [or graphene oxide (GO)] is a hydrophilic layered material produced by the oxidation of graphite [7]. Since exfoliation of graphite oxide is the only way to produce stable suspensions of quasi-two-dimensional carbon sheets, graphene oxide has attracted attention as filler for polymer nanocomposites [8]. Moreover, chemical functionalization of GO is a well established technique for obtaining nanomaterials with desired properties [9], since this can affect their dispersability and interactions with polymeric matrices [9].

In literature there is a lack of combinatory studies in polymer nanocomposites using different techniques for physical properties evaluation. In this work two series of PLLA graphene oxide nanocomposites were prepared using GO or organomodified GO. Several techniques and methods were used to evaluate the effect of the type and amount of GO on PLLA thermal transitions, molecular mobility, mechanical properties and biodegradation. The results obtained by the various techniques are critically compared and correlated to each other and discussed in terms of polymer-filler interactions and of effects of interfaces.

2. Experimental

2.1 Materials

PLLA Purasorb PL38 (inherent viscosity 3.81 dL/g, Mn=700,000 Da, water content <0.5%) was supplied by Purac Biochem (Gorinchem, The Netherlands). GO was produced through a modified Staudenmaier's method [9]. In a typical synthesis, 10 g of powdered graphite were added to a mixture of concentrated sulphuric acid and nitric acid while cooling in an ice-water bath. Potassium chlorate was added to the mixture in small portions while stirring and cooling. The reactions were quenched after 18 h by pouring the mixture into distilled water and the oxidation product was washed until pH 6. The sample was then dried at room temperature. For the synthesis of amino-functionalized GO (org-GO), 200 mg of GO were dispersed in 100 ml of water and the mixture was stirred for 1 day. A solution of 1-dodecylamine (600 mg) in ethanol (100 ml) was then added dropwise to the GO suspension and the mixture was stirred for another day. The GO derivative was isolated by centrifugation and washed three times with 1:1 (v/v) ethanol/water and then dried in air.

2.2. Preparation of the PLLA/GO and PLLA/org-GO nanocomposites

PLLA/GO and PLLA/org-GO nanocomposites were prepared using N,N-dimethylformamide (DMF) as a solvent for the dispersion of graphene and chloroform for PLLA. Proper amounts of graphene oxide were first added into DMF at a concentration of 1 mg/mL, and the mixture was stirred for 1 h to obtain a uniform dispersion. PLLA was dissolved in chloroform at a concentration of 40mg/mL. The resulting solution was mixed, stirred and sonicated for 30min with the GO dispersions at different GO loadings. The solvents were evaporated at elevated temperature for 2 days and the nanocomposite films were obtained. The filler amount was 0.5, 1 and 2.5 wt% (always referring to pure GO amount).

2.3. Wide-Angle X-ray Diffraction (WAXD) Study

The WAXD patterns of samples were collected on a D8 Advance Bruker diffractometer by using Cu Ka radiation. The patterns were recorded in the 2-theta (2Θ) range from 2 to 40°, in steps of 0.02° and counting time of 2 sec per step.

2.4. Tensile Properties

Measurements of tensile mechanical properties were performed on an Instron 3344 dynamometer, in accordance with ASTM D638, using a crosshead speed of 5 mm/min. At least five specimens were tested for each sample and the average values are reported.

2.5. Differential scanning calorimetry (DSC)

A Perkin-Elmer Diamond DSC calibrated with pure metal standards was used for studying the thermal behaviour and crystallization of the materials and in Step Scan DSC measurements.

2.6. Dielectric relaxation spectroscopy (DRS)

DRS measurements [10] were carried out by means of a Novocontrol Alpha analyzer while temperature was controlled to better than 0.5 ^{o}C by a Novocontrol Quatro cryosystem. The sample (film of 0.1 to 0.9 mm in thickness), amorphous or crystallization annnealed) was placed between the plates of a capacitor and an alternate voltage was applied in a Novocontrol sample cell. The complex dielectric permittivity, $\varepsilon^*=\varepsilon'-i\varepsilon''$, was recorded isothermally as a function of frequency in the range from 10^{-1} to 10^{6} Hz, during heating in the temperature range from -150 to 150 ^{o}C in steps of 5 or 10 ^{o}C. Measurements were performed also on amorphous polymer samples during crystallization annealing at 75 ^{o}C for a period of 2-3 h.

2.7. Polarizing Light microscopy (PLM)

A polarizing light microscope (Nikon, Optiphot-2) with a Linkam THMS 600 heating stage, a Linkam TP 91 control unit and a Jenoptic ProgRes C10Plus camera was used for PLM observations.

2.8. Enzymatic Degradation

PLLA and nanocomposite films (150±20 μm) were placed in test tubes, with 5 ml of phosphate buffer solution (0.2 M, pH=7.2) containing 0.09 mg/mL *Rhizopus delemar* lipase and 0.01 mg/mL *Pseudomonas cepacia* lipase. The loosely capped test tubes were kept at 50.0 ± 1.0 °C in an oven for 1 month while the media were replaced every 3 days. After a predetermined time the films were removed from the lipase solution, washed thoroughly with distilled water and ethanol and dried at room temperature under vacuum, till constant weight. Every measurement was repeated three times.

3. Results and Discussion

3.1. Filler dispersion and tensile properties

PLLA nanocomposites with GO or org-GO were prepared by solution casting. TEM microphotographs of the nanocomposites evidence fine dispersion especially for org-GO and low loadings (Figure 1a and b).WAXD patterns of the amorphous nanocomposites showed no peak for GO or org-GO (Figure 2a) indicating exfoliation. The patterns of the annealed samples always show the same crystal structure (Figure 1b).

Fine filler dispersion is also confirmed by the enhanced mechanical properties of the nanocomposites (table in inset to Figure 2a). Young's Modulus and tensile strength at yield and at break increase moderately in the nanocomposites, with an optimum for 1 wt% filler. The slight reduction for 2.5 wt% nanofillers, is probably due to formation of aggregates. However, even for high GO content, all values are higher than for PLLA.
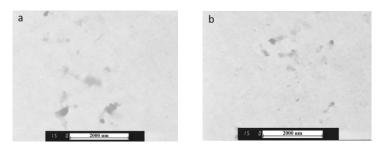
Figure 1. (a) TEM photo for PLA/GO 2.5wt% and (b) TEM photo for PLA/org-GO 2.5 wt% nanocomposites
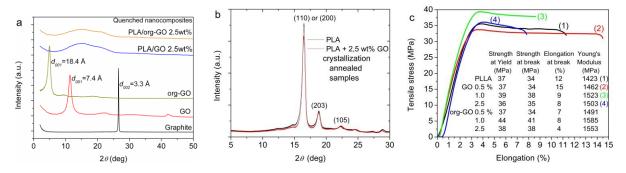

Figure 2. (a) WAXD patterns of graphite, GO, org-GO and quenched nanocomposites with 2.5 wt% GO or org-GO. (b) WAXD patterns of PLLA and PLLA/GO 2.5wt% after crystallization annealing. (c) Stress-strain curves for PLLA and PLLA/GO nanocomposites. Tensile properties are listed in the table in the inset.

Values for PLLA/org-GO nanocomposites are slightly higher than for PLLA/GO, probably due to enhanced interactions between PLLA and org-GO functionalized with amino groups. Only elongation at break seems to decrease (Figure 2c).

3.2. Crystallization and glass transition

Isothermal crystallization was faster for the nanocomposites than for neat PLLA, especially for those based on org-GO, due to stronger PLLA/org-GO interactions. Thus, the time to peak of crystallization was shorter for the nanocomposites (Figure 3a). Interestingly, the nanocomposites with 1wt% GO or org-GO showed not so fast crystallization. Low filler contents nucleate efficiently crystallization, as GO or org-GO can easier exfoliate offering more nucleation sites to the polymer. Crystallization on cooling from the melt is also faster for the nanocomposites (higher peak temperatures for given cooling rate, Figure 3b).

DSC heating scans of amorphous samples at different rates show that cold crystallization temperature (T_{cc}) decreases in the nanocomposites, indicating faster crystallization (Figure 3c). As before, for 1wt% GO or org-GO crystallization rates are not so fast. Complete exfoliation (probably for 1wt%) and formation of strong interfaces could reduce the mobility of amorphous PLLA chains and the diffusion rates needed for fast crystallization. Nanocomposites with 1wt% filler showed a distinct behavior also in their mechanical properties (Figure 2a). The fastest crystallization rates correspond to 2.5wt% filler.

Improvement in the nanocomposite properties depends on the nature and dispersion of the filler, but also on the interface adhesion strength [11]. Formation of the nanofiller-matrix interface and its effects on the amorphous phase of the composites were investigated by Step Scan DSC (MTDSC) in this section and by dielectric measurements in section 3.4.
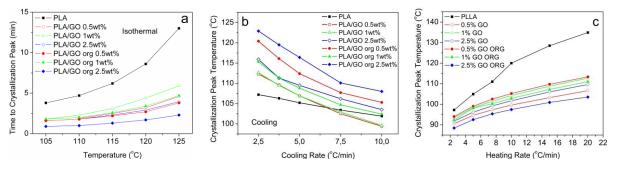
4

Figure 3. (a) Time to peak vs temperature for isothermal crystallization of PLLA and the nanocomposites. (b) T$_c$ vs cooling rate for crystallization from the melt. (c) Cold crystallization peak temperature of amorphous nanocomposites as a function of heating rate.

No substantial change in the glass transition temperature was observed in the nanocomposites by TMDSC measurements. However, the heat capacity jump at the glass transition, normalized to same amorphous fraction, ΔC_p, decreases in the nanocomposits (inset to Figure 4). These results suggest that the presence of the GO or org-GO leads to generation of an immobilized amorphous fraction in PLLA, the reduction in ΔC_p being related with the filler surface area and effective exfoliation [12]. Calculations of the immobilized amorphous fraction [12], X_{imm}, give X_{imm}=24wt% for 1wt% org-GO content compared to 11wt% for 2.5wt% org-GO content (inset to Figure 4).
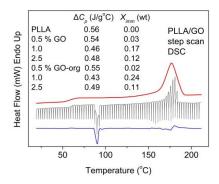

Figure 4. Step Scan DSC traces for the quenched PLLA/GO 2.5wt% nanocomposite. ΔC_p and X_{imm} values for PLLA, PLLA/GO and PLLA/org-GO nanocomposites are listed in the table in the inset.
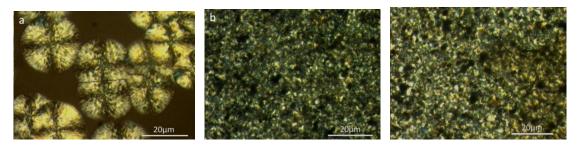

Figure 5. Spherulitic morphology of (a) neat PLLA during isothermal crystallization at 120°C, (b) PLLA/GO 0.5wt% at 125°C and (c) PLLA/org-GO 0.5wt% at 125°C

3.3. Polarized Light Microscopy (PLM)

Crystallization study by PLM showed increased nuclei density and small spherulites size in nanocomposites. Even at 125°C PLLA/GO 0.5wt% formed smaller spherulites than neat PLLA at 120°C (Figure 5). These observations prove that GO and org-GO are efficient nucleating agents.

3.4. Dielectric relaxation spectroscopy (DRS)

DRS results are shown, representatively for initial PLLA, in Figure 6a, in the form of frequency dependence of dielectric loss ε''. We focus here on segmental dynamics, i.e. on the α relaxation related to the glass transition [10]. We follow in the figure the evolution of the frequency of maximum loss and of the magnitude of the α relaxation during isothermal annealing (crystallization annealing) of PLLA every 8 min. The relaxation moves gradually towards lower frequencies and becomes weaker. The behavior has been observed before for PLLA [13] and is qualitatively similar for all the nanocomposites studied in the present work. The results were analyzed in terms of dielectric strength, $\Delta\varepsilon$, and of the frequency of loss peak, f_{max}, for the α relaxation by fitting model functions to the experimental data [12]. Using the same thermal protocol in DSC measurements we were able to follow and evaluate the gradual increasing of the degree of crystallinity, X_c, with time at 75 ^{o}C. In the inset to Figure 6a values of $\Delta\varepsilon$ for PLLA and the nanocomposites with 1 wt% GO and 1 wt% GO-org are listed at different levels of amorphous PLLA fraction (X_{amorph} i.e. 1-X_c). $\Delta\varepsilon$ is significantly lower for the nanocomposites as compared to initial PLLA, both in fully amorphous and in crystallized samples. Also, the decrease of $\Delta\varepsilon$ is stronger for the modified fillers, especially in the fully amorphous sample. These results suggest strongly that a significant amount (about 10-25wt% for PLLA/GO and 13-49wt% for PLLA/GO-org) of the polymer chains in the nanocomposites have highly reduced mobility and do not contribute to the α relaxation. Such behavior has been observed before for PLLA filled with montmorillonite nanoclays [14]. The results correlate well with the reduction of ΔC_p in the nanocomposites (DSC, Figure 4) [12, 15]. Moreover, the stronger suppression of $\Delta\varepsilon$ in PLLA/GO-org suggests that the polymer-filler interface area and/or the interaction strength are stronger, as compared to PLLA/GO, in good correlation to the result on the mechanical properties (inset to Figure 1c).
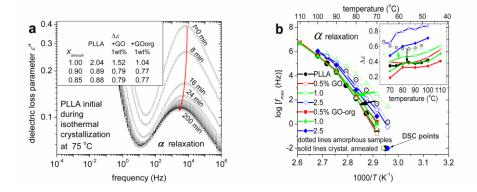

Figure 6. (a) Dielectric loss ε'' vs frequency for initial PLLA, as recorded continuously on isothermal crystallization at 75 ^{o}C. Results of the dielectric strength of α relaxation vs the amorphous polymer content, X_{amorph}, for PLLA and its nanocomposites with 1.0 wt% GO and 1.0 wt% GO-org are listed in the table in the inset. (b) Frequency maxima of segmental α relaxation for PLLA and PLLA-GO nanocomposites against reciprocal temperature (Arrhenius Plots). The inset shows the respective dielectric strength, $\Delta\varepsilon$, against temperature. The arrows indicate the changes between amorphous and fully crystalline PLLA in the samples.

Focusing now on the dynamics of the glass transition, we discuss the results of DRS measurements during heating (raw data not shown here), in the temperature range from 40 to 120 ^{o}C. By plotting f_{max} against reciprocal temperature, the Arrhenius plots for all the samples are presented in Figure 6b. One can observe immediately the expected differences between the amorphous and the (crystallization) annealed samples, where in the second case the dynamics of the α relaxation is slower [13, 15]. Regarding filler effects, it is clearly observed that the addition of GO leads systematically to faster dynamics of the α relaxation, in both

amorphous and annealed samples. Combining this observation with the previous one for the reduction of $\Delta\varepsilon$, a possible model which can describe the results is as follows: the immobilization of a polymer fraction within the GO-PLLA interface (more dense polymer conformations, as compared to the bulk [16]) could supply extra free volume in the sample, leading to easier diffusion-packing of the unaffected polymer chains [16].

Coming back to the dielectric strength, in the inset to Figure 6b, crystallization annealing suppresses $\Delta\varepsilon$. The observed increase of $\Delta\varepsilon$ at the higher loadings of GO and GO-org (inset to Figure 6b), accompanied also by an increase of the overall dielectric response (not shown), is probably an internal electric field effect [17], due to the increasing of the number of GO nanosheets and the simultaneous decreasing of the mean distance between them.

3.5. Enzymatic Degradation

Polyesters like PLLA having ester bonds can be hydrolyzed by lipases. The weight loss rates increase with the addition of filler (Figures 8a and b). Although faster hydrolysis was also observed for PLLA/org-GO nanocomposites compared with neat PLLA, the increase was not as high as in PLLA/GO nanocomposites. In nanocomposites hydrolysis is also affected by the kind and amount of nanofiller [18]. GO possess polar hydrophilic groups, like –COOH and –OH (Figure 8c) which accelerate the hydrolysis. Org-GO is less hydrophilic than GO, due to the methylene groups on its surface. Thus, PLLA/org-GO nanocomposites hydrolyze slower than PLLA/GO nanocomposites.
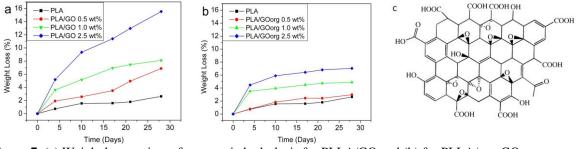

Figure 7. (a) Weight loss vs time of enzymatic hydrolysis for PLLA/GO and (b) for PLLA/org-GO nanocomposites. (c) Chemical structure of Graphene Oxide.

4. Conclusions

New nanocomposites based on PLLA, GO and organomodified GO were prepared. The crystallization and biodegradation rates of the PLLA nanocomposites increased with increasing filler content. For improved properties in nanocomposites formation of a polymer matrix/nanofiller interface is needed. The heat capacity jump at the glass transition decreased in the nanocomposites, suggesting immobilization of a polymer fraction. This explains the improvement of the mechanical properties of the nanocomposites. The improvement is maximal for 1 wt% filler, in good correlation with reduction of the heat capacity jump at T_g, and of the dielectric strength of the corresponding segmental relaxation. Compared to effects of filler content, effects of organic modification of the filler used are moderate.

Acknowledgement

References

[1] L. Yu, K. Dean, L. Li. Polymer blends and composites from renewable resources. Progress in Polymer Science, 31(6):576–602, 2006.

[2] M. Okada. Chemical synthesis of biodegradable polymers. Progress in Polymer Science, 27(1):87-133,2002.

[3] R. Sabater Serra, A. Kyritsis, J.L. Escobar Ivirico, A. Andrio Balado, J.L. Gómez Ribelles, P. Pissis, M. Salmerón-Sánchez. Structure and dynamics in poly(L-lactide) copolymer networks. Colloid and Polymer Science, 288(5):555-565, 2010.

[4] S. Sinha Ray, P. Maiti, M. Okamoto, K. Yamada, K. Ueda. New Polylactide/Layered Silicate Nanocomposites. 1. Preparation, Characterization and Properties. Macromolecules, 35(8):3104-3110, 2002.

[5] G.Z. Papageorgiou, D.S. Achilias, T. Beslikas, D.N. Bikiaris. PLA nanocomposites: Effect of filler type on non-isothermal crystallization. Thermochimica Acta, 511(1-2):129–139, 2010.

[6] A.K. Geim, K.S. Novoselov. The rise of graphene. Nature Materials, 6(3):183-191, 2007.

[7] A.B. Bourlinos, D. Gournis, D. Petridis, T. Szabo, A. Szeri, I. Dekany. Graphite oxide: Chemical reduction to graphite and surface modification with primary aliphatic amines and amino acids. Langmuir, 19(15):6050–6055, 2003.

[8] A. Enotiadis, K. Angjeli, N. Baldino, I. Nicotera, D. Gournis. Graphene-based nafion nanocomposite membranes: Enhanced proton transport and water retention by novel organo-functionalized graphene oxide nanosheets. Small, 8(21):3338-3349, 2012.

[9] D.V. Stergiou, E.K. Diamanti, D. Gournis, M.I. Prodromidis. Comparative study of different types of graphenes as electrocatalysts for ascorbic acid. Electrochemistry Communications, 12(10):1307-1309, 2010.

[10] F. Kremer, A. Schoenhals, editors. *Broadband dielectric spectroscopy*. Springer, Berlin, 2002.

[11] T. Huang, Y. Xin, T. Li, S. Nutt, C. Su, H. Chen, P. Liu, Z. Lai. Modified Graphene/Polyimide Nanocomposites: Reinforcing and Tribological Effects, ACS Appl Mater Interfaces, 5(11): 4878–4891, 2013.

[12] D. Fragiadakis, L. Bokobza, P. Pissis. Dynamics near the filler surface in natural rubber-silica nanocomposites. Polymer, 52(14):3175-3182, 2011.

[13] A.R. Bras, M.T. Viciosa, Y. Wang, M. Dionisio, J.F. Mano. Crystallization of poly(L-lactic acid) probed with dielectric relaxation spectroscopy. Macromolecules, 39(19):6513-6520, 2006.

[14] M. Pluta, J.K. Jeszka, G. Boiteux. Polylactide/montomorillonite nanocomposites: Structure, dielectric, viscoelastic and thermal properties. European Polymer Journal, 43(7):2819-2835, 2007.

[15] P. Klonos, A. Panagopoulou, L. Bokobza, A. Kyritsis, V. Peoglos, P. Pissis. Comparative studies on effects of silica and titania nanoparticles on crystallization and complex segmental dynamics in poly(dimethylsiloxane). Polymer, 51(23):5490-5499, 2010.

[16] P. Gin, N. Jiang, C. Liang, T. Taniguchi, B. Akgun, S.K. Satija, M.K. Endoh, T. Koga. Revealed architectures of adsorbed polymer chains at solid-polymer melt interfaces. Physical Review Letters, 109(26):265501, 2012.

[17] K.A. Page, K. Adachi. Dielectric relaxation in montmorillonite/polymer nanocomposites. Polymer, 47(18):6406-6413, 2006.

[18] D.N. Bikiaris. Nanocomposites of Aliphatic polyesters: An overview of the effect of different nanoparticles on enzymatic hydrolysis and biodegradation of polyesters. Polymer Degradation and Stability 98:1908-1928, 2013.